Increased extreme precipitation in Chinese deserts from 1960 to 2018

Article

Accepted Version

Increased extreme precipitation in Chinese deserts from 1960 to 2018

Guoshuai Li[1,2,3]*, Hong Yang[4], Ying Zhang[3], Chunlin Huang[3], Xiaoduo Pan[1], Mingguo Ma[5], Minhong Song[6], and Haipeng Zhao[7]

[1]Institute of Tibetan Plateau Research Chinese Academy of Sciences, Beijing, China.

[2]CAS Center for Excellence in Tibetan Plateau Earth Sciences, Beijing 100101, China.

[3]Northwest Institute of Eco-Environment and Resources, Chinese Academy of Sciences, Lanzhou, China.

[4]Department of Geography and Environmental Science, University of Reading, Whiteknights Reading, UK.

[5]Southwest University, Chongqing, China.

[6]Chengdu University of Information Technology, Chengdu, China.

[7]Indiana State University, Terre Haute, USA.

Corresponding author: Guoshuai Li (liguoshuai@itpcas.ac.cn)

Key Points:

- Increasing extreme precipitation has been observed in Chinese deserts from 1960 to 2018.
- The PRCPTOT changes and Rx1day changes in TakD, GTD, QaiD and TenD exhibit significant increasing trends.
- Wetting in the western Chinese deserts and drying in the eastern Chinese deserts are observed.

Abstract

Extreme precipitation over drylands, especially deserts, has been often observed. The precipitation changes in Chinese deserts have been rarely studied. Here, we use a daily grid precipitation dataset generated via weather station data (0.25° horizontal grid spacing) to investigate the spatial and temporal changes in extreme precipitation in Chinese deserts. The extreme precipitation based on the changes in the total precipitation (PRCPTOT) and the annual-maximum daily precipitation (Rx1day) in the Chinese desert exhibits markedly increasing trends and presents a spatial distribution of wetting in the western deserts and drying in the eastern deserts. The increase in extreme precipitation could minimize wind erosion and intensify dune stabilization in the western Chinese deserts.

1 Introduction

Desert precipitation is one of the major drivers that could influence the eco-geomorphological characteristics of dune landscape. Precipitation could improve dune ecosystems by interaction of biomass changes [*Southgate et al.*, 1996], and episodic precipitation events can increase the CO_2 flux by up to 30-fold before it returns to the background level within 48 hours [*Sponseller*, 2007]. Alternatively, precipitation events could reasonably influence the impacts of soil moisture on the wind erosion threshold before sand transport potential is restored within 12 hours [*Bergametti et al.*, 2016]. The precipitation pattern can affect the spatial distribution of the susceptibility to desert fires [*Tagestad et al.*, 2016]. The precipitation threshold can control the generation of desert ephemeral streams [*Kampf et al.*, 2018] and finally impact the runoff coefficient of desert catchments [*Zoccatelli et al.*, 2018].

Currently, most of deserts in the warm-temperature, middle-latitude zone undergo increasing precipitation. For example, the Sahel region in Africa has recently experienced increasing precipitation [*Biasutti*, 2016; *Thomas and Nigam*, 2018]. The probabilities of increasing precipitation in the extremely arid and arid regions of Chinese deserts were 83% and 70% from 1951 to 2015 [*Xu et al.*, 2008]. Studies regarding precipitation in the hinterland of individual Chinese deserts have been conducted. The hinterland of the Taklamakan Desert exhibited an increasing yearly total precipitation from 2000 to 2014 according to the records from the Tazhong weather station [*Zhou et al.*, 2017]. The hinterland of the Gurban Tunggut Desert also exhibited an increasing precipitation trend from 1996 to 2005 according to the measurements from artificial weather stations [*Sun and Yang*, 2010]. In fact, the precipitation around individual Chinese deserts also exhibited increasing trends. The precipitation around the Kumtag Desert exhibited an increasing trend from 1960 to 2014 [*Hu et al.*, 2017], and the precipitation around Badain Jaran Desert presented an increasing trend from 1971 to 2015 [*Li et al.*, 2015].

Global warming induces more frequent extreme climate events [*Diffenbaugh et al.*, 2017]. Comparisons of extreme precipitation over dryland and wetland areas have received increased attentions [*Donat et al.*, 2016; *Greve et al.*, 2014; *Polson and Hegerl*, 2016]; furthermore, extreme precipitation has been clearly linked to anthropogenic influences [*Min et al.*, 2011; *Putnam and Broecker*, 2017]. Extreme precipitation events are frequently observed in arid regions [*Donat et al.*, 2016], and deserts are typically representative of extremely arid regions. In addition, deserts generally have relatively small population; thus, the human-driven contributions to extreme precipitation events in deserts should be nonsignificant, leaving mostly natural contributions. Research on extreme precipitation in deserts can be expected to remedy the gap in the understanding of precipitation regimes in arid regions. To the best of our knowledge, extreme

precipitation based on the changes in the total precipitation (PRCPTOT) and the annual-maximum daily precipitation (Rx1day) [*Karl et al.*, 1999] in Chinese deserts have been rarely studied [*Hu et al.*, 2017], and these studies have been limited to specific deserts. This condition leads us to explore the following questions: Has precipitation increased in Chinese deserts over the last few decades? What is the degree of the response to extreme precipitation in Chinese deserts?

Here, we analyze the changes in PRCPTOT and Rx1day [*Karl et al.*, 1999] from the daily gridded precipitation dataset from 1960 to 2018, allowing for the accurate quantification of the response to the extreme precipitation in Chinese deserts under a global climate system. The precipitation indices are calculated by dividing the 30-yr average of the 1981-2010 period after subtracting the 30-yr average of this period. In this study, extreme precipitation in Chinese deserts will improve our understanding of the natural precipitation response to global climate warming in desert regions after minimizing the human-driven contributions.

2 Materials and Methods

2.1 Study area

The desert boundaries in 2013 were established with a spatial accuracy of less than 30 m using Google Earth Pro®, and changes to the desert sizes during the study period were not considered in this study. The chosen layers were from the Digital Global Features and SPOT Images, and we selected the latest time phases and the dunes without artificial interference as carefully as possible. The study areas include the Taklamakan Desert (TakD), Gurban Tunggut Desert (GTD), Qaidam Desert (QaiD), Kumtag Desert (KumD), Badain Jaran Desert (BJD), Tengger Desert (TenD), Ulan Buh Desert (UBD), Hobq Desert (HobD), MU US Sands (MUS), Hunshandake Sands (HunS), Hulunbuir Sands (HulS) and Horqin Sands (HorS) in China (Table 1 and Figure 1).

Table 1 insert here

2.2 Data and methods

In this study, the China Gauge-based Daily Precipitation Analysis (CGDPA) dataset (http://data.cma.cn/data/cdcdetail/dataCode/SEVP_CLI_CHN_PRE_DAY_GRID_0.25.html) is used to study extreme precipitation in Chinese deserts. The CGPDA dataset is from the real-time extraction of the daily precipitation amounts (08:00 – 08:00) collected by more than 2400 Chinese weather stations characterized by a spatial resolution of 0.25° and a time span of 1960 to 2018 [*Shen and Xiong*, 2016]. Additionally, a spatial resolution of 0.25° (~50 km) can adequately capture the spatial correlation of the daily precipitation amounts in deserts [*Wang et al.*, 2013].

PRCPTOT is the annual sum of the daily precipitation (≥ 1 mm), and Rx1day is the annual-maximum daily precipitation. Only the daily precipitation amounts ≥ 1 mm are used to avoid drizzle, which could cause biases in the observed data [*Zhang et al.*, 2011]. PRCPTOT change and Rx1day change are the percentages of the annual series from 1960 to 2018 after subtracting the 30-yr averages of the 1981-2010 period and dividing by the 30-yr averages of this period, see the formula:

PRCPTOT change = (yearly *PRCPTOT* from 1960 to 2018 – 30-yr average *PRCPTOT* of the 1981-2010 period) / 30-yr average *PRCPTOT* of the 1981-2010 period × 100% (1)

Rx1day change = (yearly *Rx1day* from 1960 to 2018 – 30-yr average *Rx1day* of the 1981-2010 period) / 30-yr average *Rx1day* of the 1981-2010 period × 100% (2)

The spatial distribution of linear trends is calculated using the Climate Data Operators (CDO) software [*Schulzweida*, 2019] and the temporal analysis of linear trends is derived by the XLSTAT software [*Addinsoft*, 2019].

3 Results

3.1 Spatial pattern of extreme precipitation

The spatial distribution of PRCPTOT changes in individual Chinese deserts indicates that the majority of the areas in the western deserts (e.g., TakD, GTD, QaiD, KumD, BJD and TenD) present increasing trends. In detail, an aggregated patch with increases of more than 2.1 % yr^{-1} is observed in the southern TakD, and PRCPTOT changes in the western TakD also present increasing trends greater than 1.2 % yr^{-1}. These patterns indicate that the eco-environment in the western and southwestern TakD should have improved during the study period. The PRCPTOT change trends in the southern GTD are slightly greater than those in the northern GTD. Negative PRCPTOT change trends are observed in the central QaiD and central KumD from 1960 to 2018. BJD exhibits negative to positive PRCPTOT change trends from east to west; and central-southern BJD presents positive trends greater than 0.3 % yr^{-1}, which may be related to the influence of Mount Qilian [*Li et al.*, 2015]. The majority of the area in TenD presents increasing PRCPTOT change trends. Additionally, the majority of the areas in UBD, HobD, MUS, HunS, HulS and HorS present decreasing PRCPTOT change trends from 1960 to 2018, and the trends in some grids even exceed -0.3 % yr^{-1} (Figure 1a).

The spatial distribution of the trends of the Rx1day changes are similar to those of the PRCPTOT changes, and the majority of the areas in the western deserts (e.g., TakD, GTD, QaiD, KumD, BJD and TenD) also present increasing trends. In TakD, an aggregated patch with negative Rx1day change trends less than zero is contiguous to a relatively large aggregated patch with positive trends greater than 2.1 % yr^{-1}. Both the southern GTD and eastern QaiD present positive Rx1day change trends that are greater than 1.2 % yr^{-1}. A majority of the area in KumD shows positive Rx1day change trends that are above zero. Positive Rx1day change trends greater than 0.9 % yr^{-1} are observed in the southern BJD. For TenD, positive Rx1day change trends greater than zero are observed. The Rx1day change trends in the eastern deserts (e.g., UBD, HobD, MUS, HunS, HulS and HorS) mostly fall within the range of -0.3 and 0.3 % yr^{-1}, whereas northern MUS has the lowest trends of less than -1.2 % yr^{-1} (Figure 1b).

Notably, we find a considerable increase in extreme precipitation in certain areas in the southern TakD. These increases may be related to the melting of glaciers in the Tibetan Plateau [*Brun et al.*, 2017; *Pritchard*, 2017; *Yao et al.*, 2012], the phase conversion of the Interdecadal Pacific Oscillation that resulted in the strengthened transport of water pour from the southwest towards the Tibetan Plateau [*Zhang et al.*, 2017], and large scale climate oscillation impacts in Central Asia [*de Beurs et al.*, 2018]. Besides, the spatial distribution of the PRCPTOT change trends and Rx1day change trends indicate that range of the Rx1day change trends (Figure 1b) is slightly larger than that of the PRCPTOT change trends, especially in the negative ranges (Figure 1a). Thus, more extreme precipitation was observed in Chinese deserts from 1960 to 2018.

Figure 1 insert here

3.2 Temporal distribution of extreme precipitation

The observations indicate significant linear increases in the precipitation indices in the Chinese desert (p-value < 0.05). The PRCPTOT change and Rx1day change in the Chinese desert exhibit significantly increasing trends of 0.82±0.21 % yr^{-1} and 0.52±0.17 % yr^{-1}, respectively, from 1960 to 2018, and the PRCPTOT change trend is greater than the Rx1day change trend. In brief, the precipitation increased during the study period, and the probability of occurrence of extreme precipitation also increased in the last 59-yr (Figure 2).

Figure 2 insert here

TakD is the largest desert in China and exhibits greater trends than those in other Chinese deserts. The PRCPTOT change in TakD is 1.13±0.31 % yr^{-1} (p-value = 0.001), and the Rx1day change is 0.60±0.25 % yr^{-1} (p-value = 0.020), respectively. QaiD is located in the Tibetan Plateau and has the highest elevation of all the studied Chinese deserts. The PRCPTOT change and Rx1day change exhibit significantly increasing trends in QaiD, with slopes of 0.95±0.37 % yr^{-1} (p-value = 0.013) and 0.91±0.37 % yr^{-1} (p-value = 0.018), respectively (Figure 3). In addition to TakD and QaiD, the PRCPTOT changes and Rx1day changes in GTD and TenD also present significant increasing trends during the study period (Figure 3 and Figure 4). The absolute values of the PRCPTOT change trends and Rx1day change trends in the western deserts (e.g., TakD, GTD, QaiD, KumD, BJD and TenD) are obviously greater than those in the eastern deserts (e.g., UBD, HobD, MUS, HunS, HulS and HorS) during the study period (Figure 3 and Figure 4). The minimum absolute PRCPTOT change trend is approximately zero in HulS, which indicates that the precipitation in HulS is evenly distributed throughout the study period. Thus, the Rx1day change in HulS indicates a nonsignificant decreasing trend.

Figure 3 insert here

Figure 4 insert here

3.3 Trend uncertainties

The uncertainties in the PRCPTOT change trends and Rx1day change trends mainly incorporate (1) variability among the different years used to calculate the trends from 1960 to 2018 (solution uncertainty); and (2) uncertainty in the trend (slope of the linear regression) based on linear regression (trend uncertainty).

To estimate the solution uncertainty, we calculated the ensemble standard deviations of the annual series of the PRCPTOT changes and Rx1day changes from 1960 to 2018 (Figure 5), wherein 1 std. is used to represent solution uncertainty (the mean ± 1 std.) (Figure 2-4). Trend uncertainty reflects the uncertainty in the slopes from the linear regression analysis, wherein 1 s.e. is used to represent trend uncertainty (the slope ± 1 s.e.) (Figure 2-4).

Figure 5 insert here

The values of the PRCPTOT change std. are above 40% for the majority of the areas in TakD, QaiD and KumD from 1960 to 2018. Existing aggregated patches of PRCPTOT changes in the southern TakD, northern QaiD and central KumD have high std. values, and some grids even exceed 110%. The majority of the areas in GTD and TenD have PRCPTOT change std. values of less than 50%. Although the PRCPTOT change std. values are greater than 60% in the northern BJD, the values are less than 40% in the southern BJD. This limited variability may result from the influence by Mount Qilian [*Li et al.*, 2015]. The majority of the areas in UBD, HobD, MUS, HulS and HorS have PRCPTOT change std. values of less than 50%, and these low values may be related to the larger number of weather stations in the eastern deserts [*Shen et al.*, 2010]. Different from the PRCPTOT change std. values in the eastern HunS, PRCPTOT change std. values in the western HunS are as high as 80%.

The spatial distribution of the Rx1day change std. values indicates that the Rx1day change std. values exceed 100% in some areas of the TakD, QaiD and KumD, and these values correspond to the spatial distribution of the PRCPTOT change std. values in these deserts. A majority of the area in GTD has Rx1day change std. value of less than 60%. Similar to the PRCPTOT change std. values in BJD, the Rx1day change std. values in the southern BJD are still lower than those in the northern BJD. A majority of the area in TenD has Rx1day change std. values of less than 60%, except for some of the areas where the std. values are greater than 80%. The eastern deserts (e.g., UBD, HobD, MUS, HulS and HorS) mainly have Rx1day change std. values of less than 60%, except for the Rx1day change std. values of up to 260% of that are observed in the western HunS.

Although few weather stations are available in most of the deserts, existing studies have shown that the yearly, monthly and seasonal precipitation distribution in the hinterland of some deserts are basically in accordance with those measured by the weather stations around the deserts [*Sun and Yang*, 2010; *Zhou et al.*, 2017]. Additionally, 0.25° (~50 km) is the threshold distances that could capture the spatial correlation of the daily precipitation amounts in deserts [*Wang et al.*, 2013]. Therefore, in this study, a modified climatology-based optimal interpolation with topographic correction used in CGDPA [*Shen and Xiong*, 2016; *Xie et al.*, 2007] is suitable for studying desert precipitation, not excluding the introduction of interpolation errors.

4 Conclusions

The spatial and temporal distribution of the PRCPTOT change trends and Rx1day change trends show that the Chinese desert exhibited more extreme precipitation from 1960 to 2018. In individual Chinese deserts, the PRCPTOT changes and Rx1day changes exhibit significant (p-value < 0.05) increasing trends in only TakD, QaiD, GTD and TenD. Both the PRCPTOT changes and Rx1day changes in the western deserts (e.g., TakD, GTD, QaiD, KumD, BJD and TenD) exhibit increasing trends, and those in the eastern deserts (e.g., UBD, MUS, HulS and HorS) exhibit decreasing trends. The PRCPTOT changes in HobD and HorS present decreasing trends; however, the Rx1day changes in these two deserts exhibit decreasing but nonsignificant (p-value > 0.9) trends.

River runoff continuously increased due to glacier melting in western China [*Ragettli et al.*, 2016; *Shi et al.*, 2007], and the acceleration of the local water cycle and intensification of the westerly belt [*Yao et al.*, 2012] may trigger an atmospheric river [*French et al.*, 2018; *Waliser*

and Guan, 2017], which may induce increasing PRCPTOT change trends and Rx1day change trends in the western deserts (e.g., TakD, GTD, QaiD, KumD, BJD and TenD). Additionally, the implementation of ecosystem service programmes, such as the Natural Forest Conservation Program (NFCP) and the Sloping Land Conversion Program (SLCP) shelter forest projects by the Chinese government [*Ouyang et al.*, 2016], and the increase in effective environmental protection measures [*Fu*, 2008; *Yang*, 2014] improve the eco-environment in the western deserts and finally contribute to increasing extreme precipitation in the Chinese desert.

Increased precipitation in deserts could effectively reduce wind erosion [*Bergametti et al.*, 2016], and could even result in the greening of deserts; furthermore, these changes could restrain the deterioration of dune ecosystems. However, the decrease in the amount of ejected dust particles by the increased extreme precipitation in deserts could inhibit the generation of precipitation [*Rosenfeld et al.*, 2001], reduce precipitation accumulation in the High Asia mountain glaciers, accelerate the glacier melting process and worsen the environmental change around the Tibetan Plateau region. The superimposed effects induced by increases in extreme precipitation in Chinese deserts should be further studied in the future.

Acknowledgments

This research is supported jointly by the Strategic Priority Research Program of the Chinese Academy of Sciences, Grant No. XDA19040504 and the National Natural Science Foundation of China, Grant No. 41471292, 41871250 and Y911171001.All processed data about extreme precipitation in Chinese deserts are archived: https://doi.pangaea.de/10.1594/PANGAEA.900083. We thank Ningke Hu, Xuehong Bai and Xiaojie Zhao for their help with desert boundary processing, and thank Xin Li for help with language editing.

References

Addinsoft, 2019. XLSTAT statistical and data analysis solution, Long Island, NY, USA.

Bergametti, G., Rajot, J. L., Pierre, C., Bouet, C. and Marticorena, B., 2016. How long does precipitation inhibit wind erosion in the Sahel? Geophys. Res. Lett., 43(12): 2016GL069324, doi: 10.1002/2016GL069324.

Biasutti, M., 2016. What brings rain to the Sahel? Nat. Clim. Chang., 6: 897, doi: 10.1038/nclimate3080.

Brun, F., Berthier, E., Wagnon, P., Kääb, A. and Treichler, D., 2017. A spatially resolved estimate of High Mountain Asia glacier mass balances from 2000 to 2016. Nature Geoscience, 10: 668, doi: 10.1038/ngeo2999.

de Beurs, K. M., Henebry, G. M., Owsley, B. C. and Sokolik, I. N., 2018. Large scale climate oscillation impacts on temperature, precipitation and land surface phenology in Central Asia. Environmental Research Letters, 13(6): 065018, doi: 10.1088/1748-9326/aac4d0.

Diffenbaugh, N. S. et al., 2017. Quantifying the influence of global warming on unprecedented extreme climate events. Proc. Natl. Acad. Sci. USA, 114(19): 4881-4886, doi: 10.1073/pnas.1618082114.

Donat, M. G., Lowry, A. L., Alexander, L. V., Ogorman, P. A. and Maher, N., 2016. More extreme precipitation in the world's dry and wet regions. Nature Clim. Change, 6(5): 508-513, doi: 10.1038/nclimate2941.

French, J. R. et al., 2018. Precipitation formation from orographic cloud seeding. Proc. Natl. Acad. Sci. USA, 115(6): 1168-1173, doi: 10.1073/pnas.1716995115.

Fu, B., 2008. Blue Skies for China. Science, 321(5889): 611-611, doi: 10.1126/science.1162213.

Greve, P. et al., 2014. Global assessment of trends in wetting and drying over land. Nature Geosci, 7(10): 716-721, doi: 10.1038/ngeo2247.

Hu, Y. et al., 2017. Temporal and spatial variability of the extreme precipitation around the Kumtag Desert. Journal of Desert Research, 37(3): 536-545.

Kampf, S. K. et al., 2018. Rainfall thresholds for flow generation in desert ephemeral streams. Water Resources Research, 54(12): 9935-9950, doi: doi:10.1029/2018WR023714.

Karl, T. R., Nicholls, N. and Ghazi, A., 1999. CLIVAR/GCOS/WMO Workshop on Indices and Indicators for Climate Extremes Workshop Summary. In: Karl, T. R., Nicholls, N. and Ghazi, A. (Editors), Weather and Climate Extremes: Changes, Variations and a Perspective from the Insurance Industry. Springer Netherlands, Dordrecht, pp. 3-7.

Li, W., Lu, S., Dong, Z., Fan, G. and Chen, L., 2015. Spatial and temporal variation of precipitation over areas surrounding the Badan Jaran Desert. Journal of Desert Research, 35(1): 94-105.

Min, S.-K., Zhang, X., Zwiers, F. W. and Hegerl, G. C., 2011. Human contribution to more-intense precipitation extremes. Nature, 470(7334): 378-381, doi: 10.1038/nature09763.

Ouyang, Z. et al., 2016. Improvements in ecosystem services from investments in natural capital. Science, 352(6292): 1455-1459, doi: 10.1126/science.aaf2295.

Polson, D. and Hegerl, G. C., 2016. Strengthening contrast between precipitation in tropical wet and dry regions. Geophys. Res. Lett.: 2016GL071194, doi: 10.1002/2016GL071194.

Pritchard, H. D., 2017. Asia's glaciers are a regionally important buffer against drought. Nature, 545(7653): 169-174, doi: 10.1038/nature22062.

Putnam, A. E. and Broecker, W. S., 2017. Human-induced changes in the distribution of rainfall. Science Advances, 3(5), doi: 10.1126/sciadv.1600871.

Ragettli, S., Immerzeel, W. W. and Pellicciotti, F., 2016. Contrasting climate change impact on river flows from high-altitude catchments in the Himalayan and Andes Mountains. Proc. Natl. Acad. Sci. USA, 113(33): 9222-9227, doi: 10.1073/pnas.1606526113.

Rosenfeld, D., Rudich, Y. and Lahav, R., 2001. Desert dust suppressing precipitation: A possible desertification feedback loop. Proceedings of the National Academy of Sciences, 98(11): 5975-5980, doi: 10.1073/pnas.101122798.

Schulzweida, U., 2019. CDO User Guide (Version 1.9.6).

Shen, Y., Feng, M., Zhang, H. and Gao, F., 2010. Interpolation Methods of China Daily Precipitation Data. Journal of Applied Meteorolgical Science, 21(3): 279-286.

Shen, Y. and Xiong, A., 2016. Validation and comparison of a new gauge-based precipitation analysis over mainland China. Int. J. Climatol., 36(1): 252-265, doi: 10.1002/joc.4341.

Shi, Y. et al., 2007. Recent and Future Climate Change in Northwest China. Climatic Change, 80(3): 379-393, doi: 10.1007/s10584-006-9121-7.

Southgate, R. I., Masters, P. and Seely, M. K., 1996. Precipitation and biomass changes in the Namib Desert dune ecosystem. Journal of Arid Environments, 33(3): 267-280, doi: https://doi.org/10.1006/jare.1996.0064.

Sponseller, R. A., 2007. Precipitation pulses and soil CO2 flux in a Sonoran Desert ecosystem. Global Change Biology, 13(2): 426-436, doi: doi:10.1111/j.1365-2486.2006.01307.x.

Sun, D. and Yang, J., 2010. Precipitation characteristics at the hinterland of Gurbantunggut Desert and the surrounding areas. Arid Land Geography, 33(5): 769-774.

Tagestad, J., Brooks, M., Cullinan, V., Downs, J. and McKinley, R., 2016. Precipitation regime classification for the Mojave Desert: Implications for fire occurrence. Journal of Arid Environments, 124: 388-397, doi: https://doi.org/10.1016/j.jaridenv.2015.09.002.

Thomas, N. and Nigam, S., 2018. Twentieth-Century Climate Change over Africa: Seasonal Hydroclimate Trends and Sahara Desert Expansion. J. Clim., 31(9): 3349-3370, doi: 10.1175/jcli-d-17-0187.1.

Waliser, D. and Guan, B., 2017. Extreme winds and precipitation during landfall of atmospheric rivers. Nature Geosci, 10(3): 179-183, doi: 10.1038/ngeo2894.

Wang, N. a. et al., 2013. A preliminary study of precipitation characteristics in the hinterland of Badain Jaran desert. Advances in Water Science, 24(2): 153-160.

Xie, P. et al., 2007. A gauge-based analysis of daily precipitation over East Asia. Journal of Hydrometeorology, 8(3): 607-626, doi: 10.1175/jhm583.1.

Xu, L., Zhou, H., Li, Y., Li, H. and Tang, Y., 2008. Analysis of the precipitation stability and variety trend in the desert region of northern China. Advances in Water Science, 19(6): 792-799.

Yang, H., 2014. China must continue the momentum of green law. Nature, 509: 535-535.

Yao, T. et al., 2012. Different glacier status with atmospheric circulations in Tibetan Plateau and surroundings. Nature Clim. Change, 2(9): 663-667, doi: 10.1038/nclimate1580.

Zhang, W., Zhou, T. and Zhang, L., 2017. Wetting and greening Tibetan Plateau in early summer in recent decades. Journal of Geophysical Research: Atmospheres, 122(11): 5808-5822, doi: 10.1002/2017JD026468.

Zhang, X. et al., 2011. Indices for monitoring changes in extremes based on daily temperature and precipitation data. Wiley Interdisciplinary Reviews: Climate Change, 2(6): 851-870, doi: 10.1002/wcc.147.

Zhou, C. et al., 2017. Characteristics of precipitation at the hinterland of the Taklimakan Desert. Journal of Desert Research, 37(2): 343-348.

Zoccatelli, D. et al., 2018. Contrasting rainfall-runoff characteristics of floods in Desert and Mediterranean basins. Hydrol. Earth Syst. Sci. Discuss., 2018: 1-18, doi: 10.5194/hess-2018-550.

Table 1. Statistics of individual Chinese deserts

Full name	Abbreviation	West	North	East	South	Geodesic area (10^3km^2)
Taklamakan Desert	TakD	76.344°E	41.837°N	91.839°E	36.415°N	386.490
Gurban Tunggut Desert	GTD	82.629°E	46.556°N	91.715°E	44.070°N	63.194
Qaidam Desert	QaiD	90.092°E	38.998°N	98.234°E	36.018°N	49.302
Kumtag Desert	KumD	90.480°E	42.338°N	94.642°E	39.129°N	23.038
Badain Jaran Desert	BJD	99.371°E	42.271°N	106.151°E	38.407°N	73.681
Tengger Desert	TenD	102.783°E	39.998°N	105.667°E	37.426°N	41.813
Ulan Buh Desert	UBD	105.028°E	40.920°N	106.995°E	38.884°N	12.268
Hobq Desert	HobD	107.196°E	40.817°N	111.228°E	39.740°N	10.135
MU US Sands	MUS	107.409°E	39.416°N	110.287°E	37.563°N	24.717
Hunshandake Sands	HunS	111.769°E	43.625°N	117.499°E	42.403°N	22.395
Hulunbuir Sands	HulS	117.892°E	49.422°N	119.578°E	47.529°N	3.421
Horqin Sands	HorS	118.111°E	44.509°N	122.047°E	42.747°N	7.985

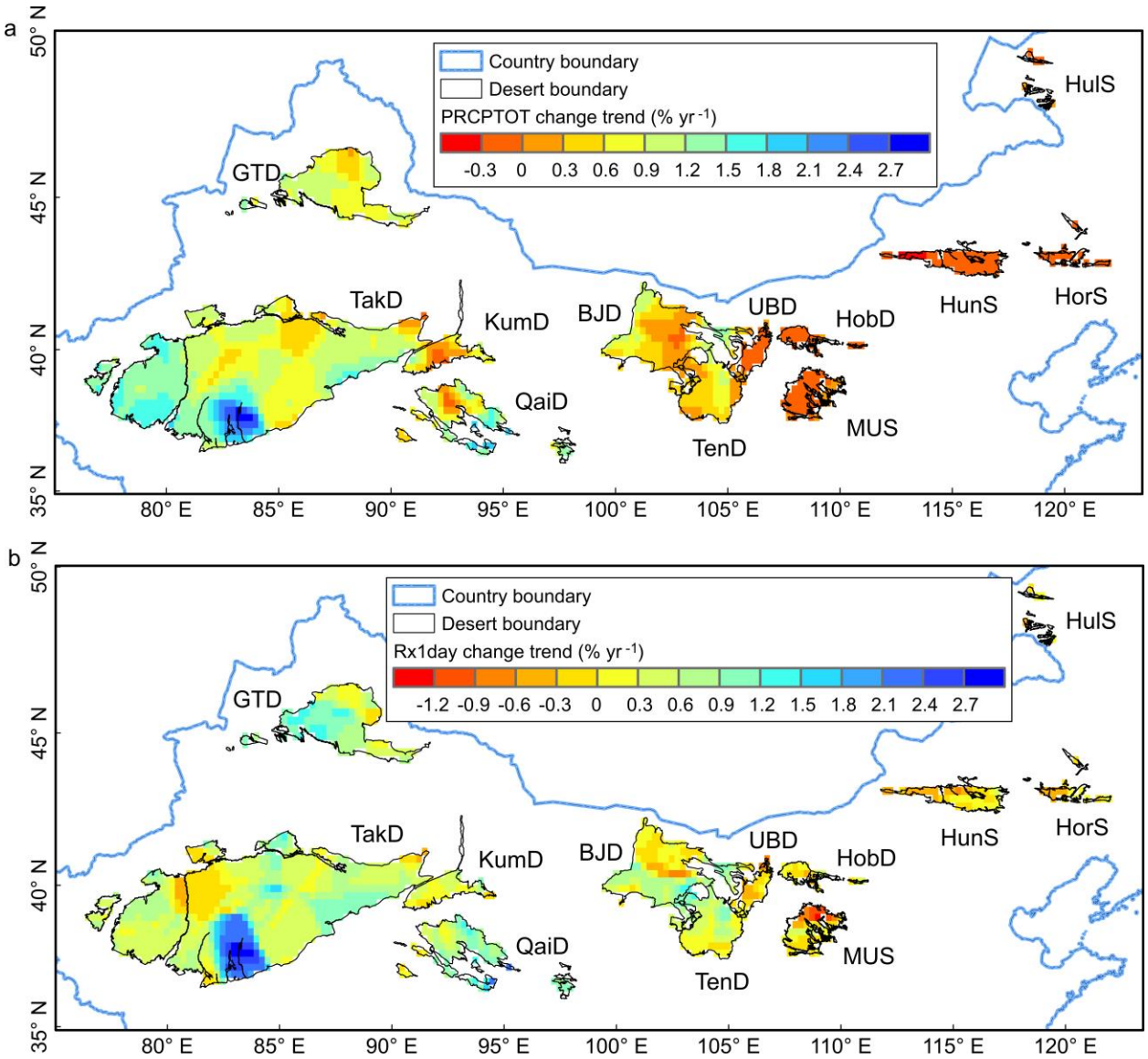

Figure 1. Trends of precipitation indices in Chinese deserts from 1960 to 2018

The spatial distributions of the PRCPTOT changes (Figure 1a) and Rx1day changes (Figure 1b) are based on the 30-yr average precipitation indices of the 1981-2010 period in Chinese deserts. The spatial distribution of the trends is based on the linear regression fit, with red representing a decrease and blue representing an increase, and the spacings are maintained at 0.3%. Characters such as TakD are the abbreviations of individual deserts in China (Table 1).

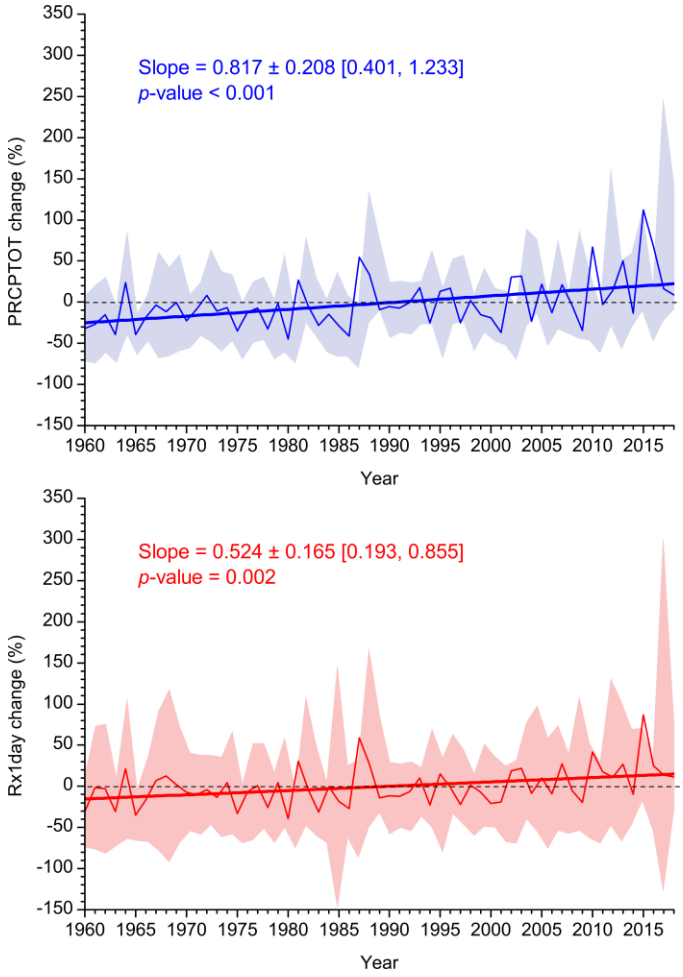

Figure 2. PRCPTOT change and Rx1day change in the Chinese desert from 1960 to 2018.

The calculations of both precipitation indices are based on the 1981-2010 period. The blue curve represents the annual series of the PRCPTOT change from 1960 to 2018, with the blue shading indicating the range of the mean ± 1 standard deviation (std.). Likewise, the red curve represents the annual time series of the Rx1day change from 1960 to 2018, with the red shading indicating the range of the mean ± 1 std.. The slope is the linear trend estimate (unit, % yr^{-1}), which indicates the slope ± 1 standard error (s.e.) of the linear trend. The *p*-value is the significance of the trend derived from a linear trend test; the first and second values in the square brackets are the lower (95%) and upper (95%) bounds of the slope, respectively.

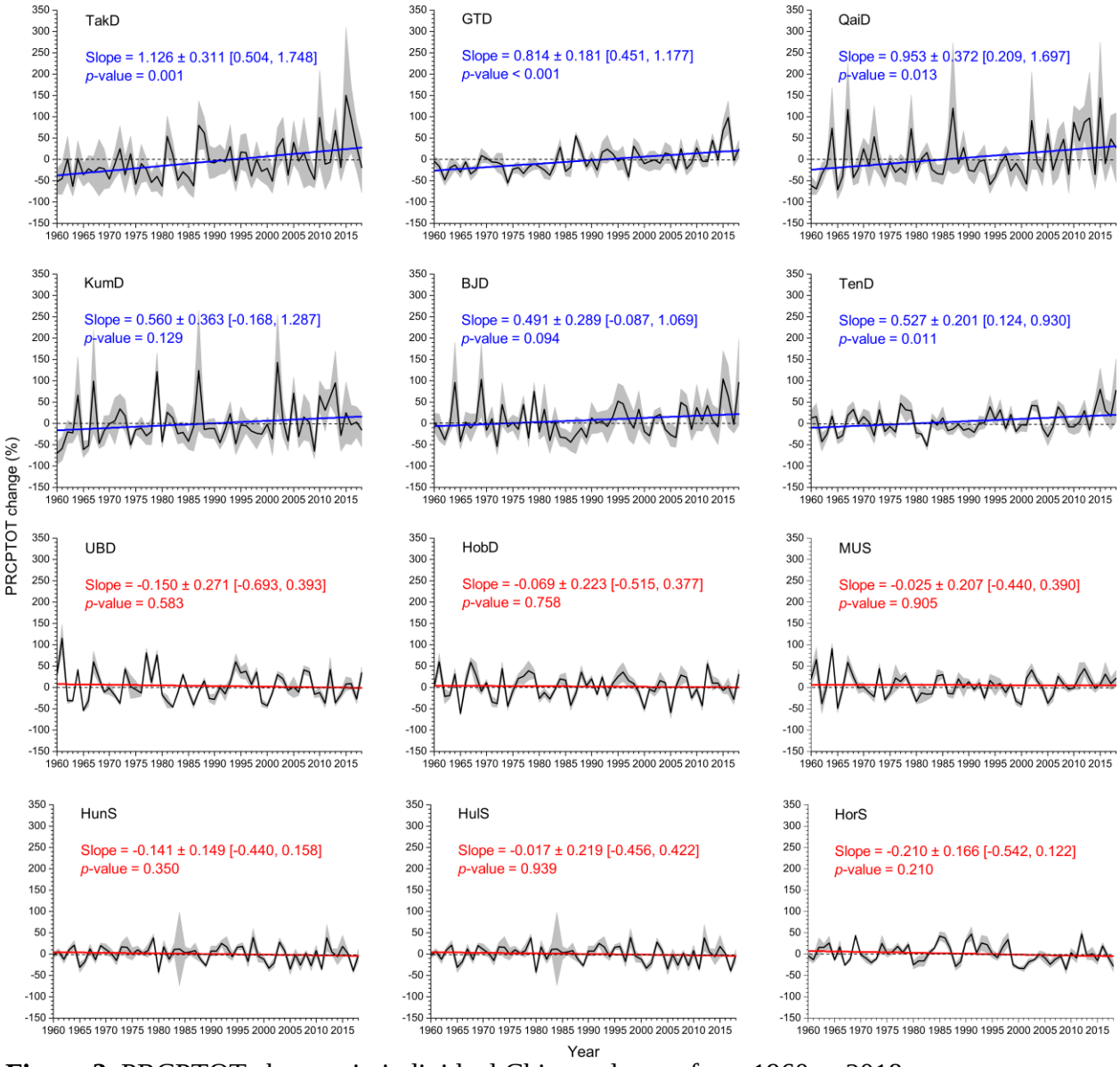

Figure 3. PRCPTOT changes in individual Chinese deserts from 1960 to 2018

The calculations of the PRCPTOT changes were based on the 1981-2010 period. The black curve represents the annual series of PRCPTOT changes from 1960 to 2018, with grey shading indicating the range of the mean ± 1 std.. The solid blue line represents the best linear fit for the increasing trend, and the solid red line represents the best linear fit for the decreasing trend. The slope is the linear trend estimate (unit, % yr^{-1}), showing the slope ± 1 s.e. of the linear trend; and the *p*-value is the significance of the trends derived from a linear trend test. The first and second values in the square brackets are the lower (95%) and upper (95%) bounds of the slope, respectively. See Table 1 for the definitions of the abbreviation such as TakD.

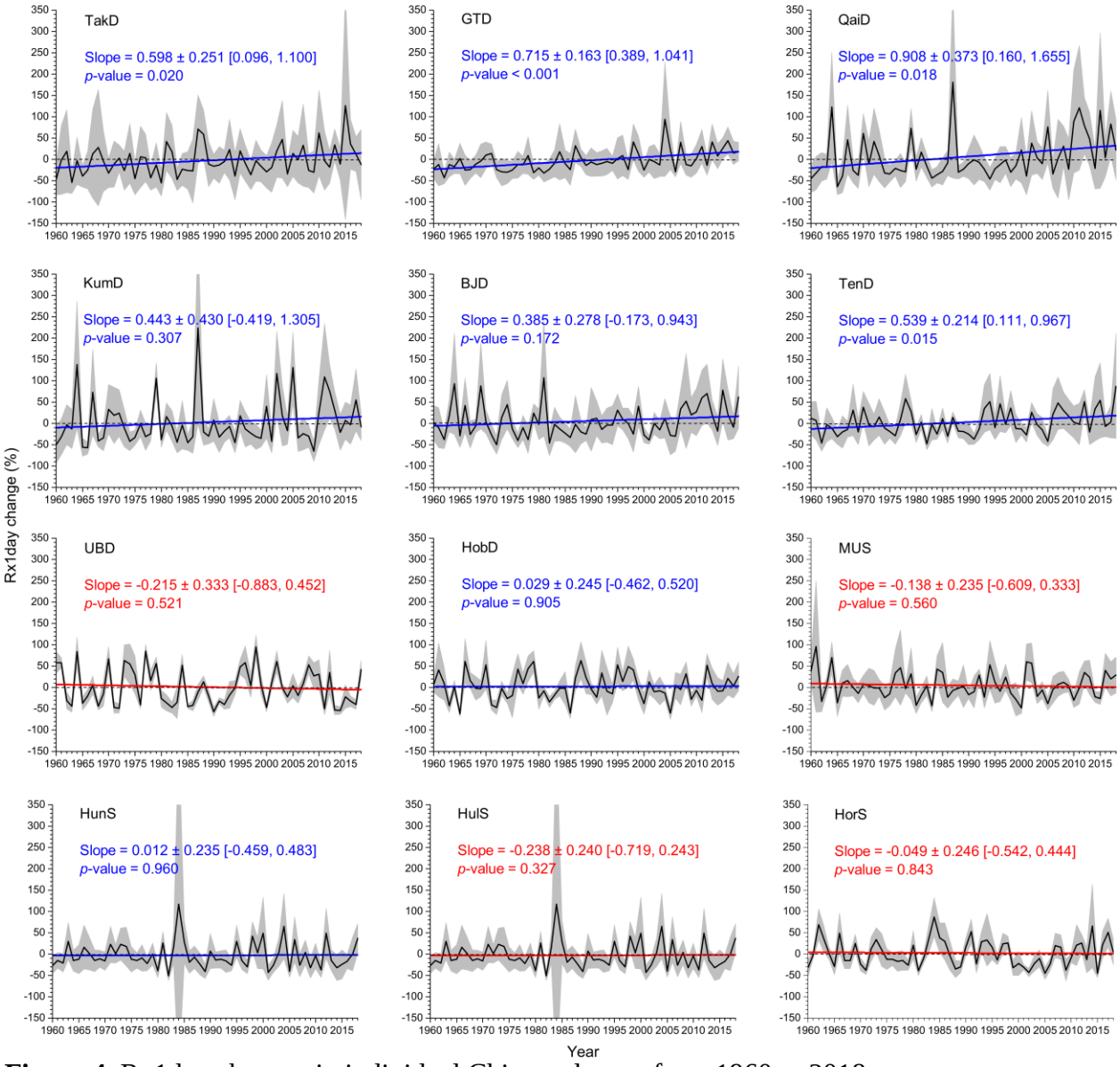

Figure 4. Rx1day changes in individual Chinese deserts from 1960 to 2018

The same as Figure 3 but for Rx1day changes.

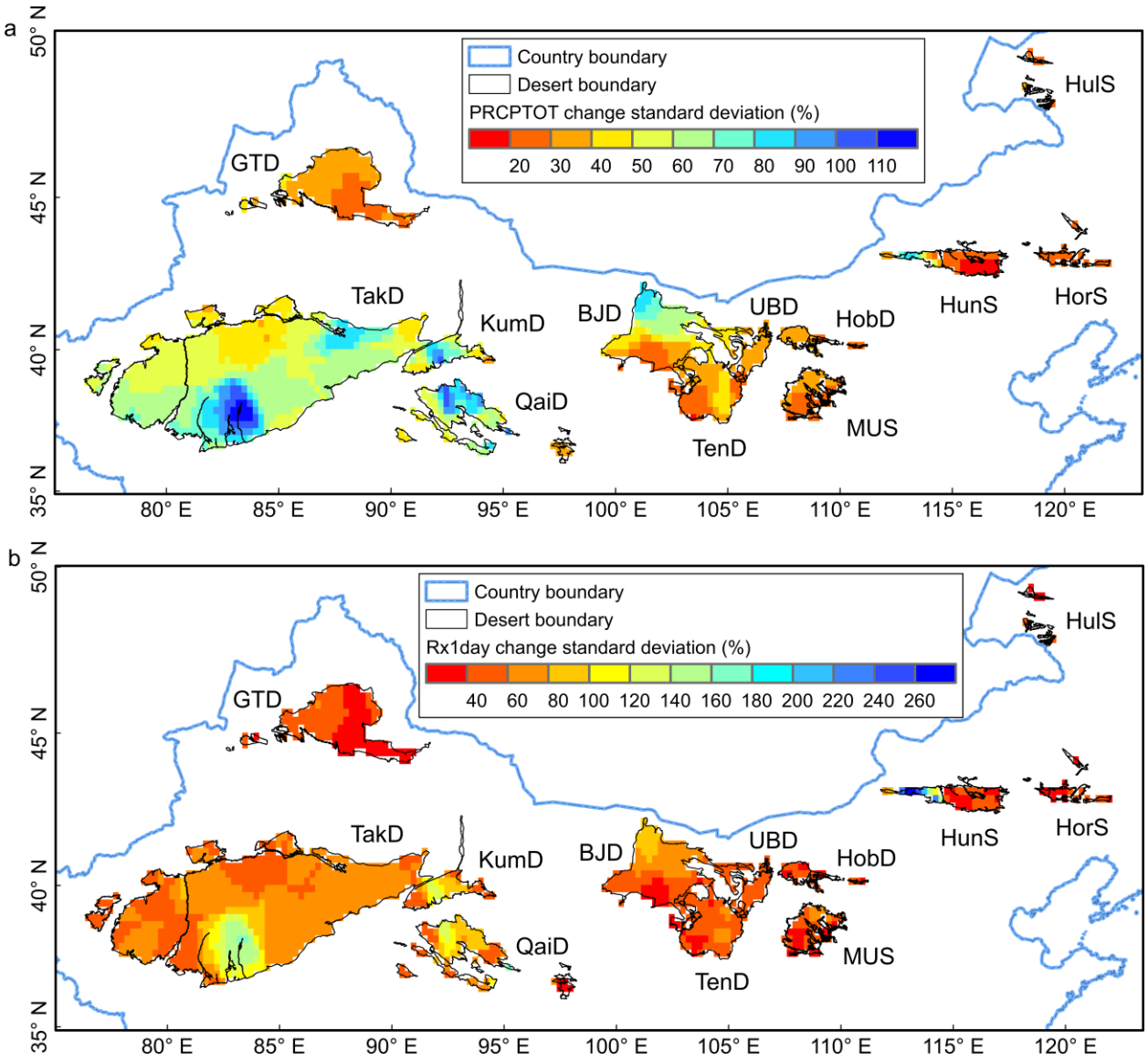

Figure 5. Calculation uncertainty of precipitation indices in Chinese deserts from 1960 to 2018

The spatial distributions of the std. of the calculation uncertainty of the PRCPTOT changes (Figure 5a) and Rx1day changes (Figure 5b) are based on the 30-yr average precipitation indices of the 1981-2010 period in Chinese deserts. The PRCPTOT change std. and Rx1day change std. are the ensemble standard deviations from the annual series of PRCPTOT changes and Rx1day changes from 1960 to 2018, and the divisor is 59. Red represents a decrease, and blue represents an increase. Spacings of 10% and 20% correspond to the PRCPTOT change std. and Rx1day change std., respectively. Characters such as TakD are the abbreviations of individual deserts in China.